Effects of different tilt-angle distributions and ambient pressures on the acoustic target strength of capelin (*Mallotus villosus*)

Roar Jørgensen and Kjell Kristian Olsen

Norwegian College of Fishery Science, University of Tromsø, N-9037 Tromsø, Norway.

Abstract

Acoustic backscattering characteristics of capelin when swimming at different depth have been investigated in a submersible experimental rig with a 38-kHz split-beam echo sounder system. The experimental system made it possible to separate the effects of swimbladder compression at various depths (5, 20 and 40 m) from the effect of changes in swimming behaviour (tilt angle). The experiments in the submersible rig demonstrate that the acoustic target strength of capelin depends on tilt angle distribution and ambient pressure. The findings indicate that differences in vertical distribution of capelin in different areas and seasons, or between years with differences in oceanographic conditions or predation, may significantly influence absolute estimates of stock abundance of capelin.

Key words: Capelin, saithe, target strength, depth, pressure, tilt angle.

Corresponding author: Roar Jørgensen, Norwegian College of Fishery Science, University of Tromsø, N-9037 Tromsø, Norway. Tel: +47 77 64 60 84, fax: +47 77 64 60 20, e-mail: roarj@nfh.uit.no.

Introduction

The capelin (*Mallotus villosus*) is a small pelagic planktivorous fish with a circumpolar Arctic distribution (Carscadden and Vilhjálmsson, 2002). The Barents Sea capelin stock is surveyed every autumn and the abundance is estimated by use of acoustic methods. The resulting stock size estimate is the basis of an assessment model (Gjøsæter *et al.,* 2002) that is used by ICES to provide advice on regulation of the fishery.

Capelin belong to the family Osmeridae and have a physostomous gas bladder with limited or no ability for gas secretion (Fahlèn, 1968). Capelin often undertake considerable vertical migrations, which apparently should lead to both compression of the swimbladder and to hydrostatic under-buoyancy. Both of these effects are expected to have an impact on the acoustic backscattering of capelin and may lead to differences in estimated abundance when the capelin is positioned at different depths (Shackell *et al*., 1994).

The acoustic target strength (TS) expresses the acoustic backscattering cross section (σ_{bs}) of the fish in decibels (dB):

$$TS = 10 \log_{10}(\sigma_{bs}) \qquad \text{(MacLennan } et\ al.,\ 2002) \qquad (1)$$

The TS is related to the length through TS equations, which assumes an average depth distribution and behaviour (Foote, 1987a). For Barents Sea capelin, the commonly used equation (Toresen *et al*., 1998) was derived from measurements of maximum TS (Dalen *et al*., 1976) and mean TS estimated by echo trace counting and echo integration (Midttun and Nakken, 1971; 1977; Dommasnes and Røtingen, 1984). The equation is expressed as:

$$TS = 19.1 \log_{10}(\text{length cm}) - 74 \quad (2)$$

Olsen and Ahlquist (1989) observed reductions (1 – 1.5 dB) in TS when capelin were lowered from depths of 5 to 50 m in cage experiments. In another physostomous species, herring (*Clupea harengus*), Ona (2003) has demonstrated an even more dramatic effect of pressure on TS at greater depths. When ambient pressure increases without gas being secreted into the swimbladder, this may deform the swimbladder and affect the backscattering directivity pattern (Mukai and Iida, 1996; Olsen and Ahlquist, 1996; Gorska and Ona, 2003). This may also lead to a state of hydrostatic under-buoyancy of the fish, which may again influence the swimming behaviour, perhaps through a more positive (headup) average tilt orientation.

The vertical migration of immature and adult capelin changes in the course of the year (Gjøsæter, 1998). In spring (March to April), when light reappears after the polar night, the capelin descend to the near-bottom layers at sunrise, but ascend at the onset of twilight. In summer (May-August) when the light lasts for 24 hours, the vertical migration becomes less distinct. In September, when the changes in light intensity between day and night become more clear-cut, the diurnal rhythm of vertical migration reappears. This variation in diurnal vertical migration may have an impact on acoustic abundance estimation (Shackell *et al.,* 1994).

This paper reports some experimental results on adult capelin where TS has been measured at different tilt angles and at modest differences in ambient pressure. The effects of different tilt angle distributions and ambient pressures on the acoustic backscattering cross-section and the practical effect for different behavioural scenarios are discussed.

Materials and methods

Experimental setup

TS experiments were carried out in Ramfjord, a sheltered fjord in North Norway. The experimental setup is shown in Figure 1. The measuring rig consists of a steel frame, combined with a curved track for an electric winch-driven "transducer wagon" for carrying a 38-kHz split-beam echo sounder transducer. The 38-kHz echo sounder system is operated at 1 ms pulse duration, medium bandwidth and 0.2 s ping interval (SIMRAD, 1999). The transducer wagon can be moved slowly along the curved track, focusing the 12.5° sound beam on the centre of a fish cage suspended at 4 m distance. The transducer displacement thus makes possible an up to 46° change of observation angle of a fish target in the cage, and the sector can be covered repeatedly by moving the transducer wagon down and up.

The rig is suspended by a wire from the vessel derrick and can be lowered and towed slowly ahead in an approximate stable vertical position. The net cage is kept in correct position by a nylon gut suspension system, including two vertical steel tubes attached to the steel frame which is positioned in a minimum zone outside the main lobe of the acoustic beam (Figure 1, right panel). The fish is placed inside the net cage and swims towards the current when the rig is towed ahead. The behaviour of the fish is monitored by an underwater television (UTV) attached to one of the vertical steel tubes and is recorded on video. The underwater cameras used were an OSPREY OE 1324 in 2001 and an OSPREY OE 1360 in 2002. The towing speed is adjusted in order to maintain the approximate normal cruising speed of the fish, but due to variable currents, the swimming speed may vary between 0.2 to 0.5 ms^{-1}. A current meter attached on the rig measures the towing speed. The cage is 45 cm long, 20 cm wide and 20 cm high and is constructed of multifilament nylon with a mesh size of 10 mm. The time of the video and echo sounder recordings is synchronised.

Complete calibrations of the 38-kHz split beam echo sounder system was done during earlier net pen experiments (Jørgensen, 2003). Additional performance tests in the actual measuring situation in the rig were performed at 5, 20 and 40 m depths by placing a 60-mm copper sphere in the centre of the cage (see Appendix A). Figure 2 shows the TS of the copper sphere and the empty cage at different observation angles. The measured TS of the copper sphere decreases with depth due to pressure effects on the transducer (about 0.5 and 0.8 dB at 20 and 40 m depths, respectively). The estimated deviation from the theoretical TS value (-33.6 dB) of the copper sphere was added to the fish measurements to account for the pressure effects on the transducer.

The experimental setup was thoroughly tested on small saithe (*Pollachius virens*) prior to the measurements on capelin. TS measurements on capelin were performed on 10 mature specimens (17.5 to 19.6 cm). The capelin had been caught by pelagic trawl during the spawning migration in 2002 and stored for seven weeks in tanks at the Tromsø Aquaculture Research Station. They were fed until they were transferred to tanks on board RV Johan Ruud prior to the TS measurements.

Analysis of target strength and tilt angle data

A calibrated split-beam echo sounder system enables detection of the position of a target within the acoustic beam and makes direct TS measurements. The position is given as range from the transducer and as alongship and athwartship angles in relation to the beam axis. Data acquisition was limited to targets with normalised echo lengths between 0.8 and 1.8 ms, target position gain compensation < 6.0 dB and maximal phase deviation 10.0 steps (SIMRAD, 1999), and with the minimum TS values equal to –65 dB. At rather extreme observation

angles, the TS of the fish became rather low, sometimes less than 10 dB stronger than the TS of the cage, and the single-fish detection algorithms in the echo sounder system occasionally failed to detect the echo from the fish as a single target. Totally, the echoes of the capelin (17.5 to 19.6 cm) were detected in 79-90% of the transmissions. Because the fish and the copper sphere were always positioned close to the centre of the beam, "undetected" TS values could be roughly estimated from the volume backscattering coefficient of the fish ($s_{v\ fish}$) and the copper sphere ($s_{v\ sphere}$).

$$TS = 10 \log (s_{v\ fish} / s_{v\ sphere}) + TS_{sphere} \qquad (3)$$

where TS_{sphere} is the TS of the copper sphere (-33.6 dB).

The swimming angles of the fish in relation to the rig were measured from videotape images with two-second intervals (see Appendix B for details), which corresponds to 1.2 images per degree change in observation angle. As the transducer wagon passed along the curved track, the time series of video images had a rather low sampling rate (0.5 s^{-1}) as compared to the time series of TS measurements (5 s^{-1}). Therefore, the time series of measured swimming angles were interpolated by linear interpolation to the same length as the TS time series.

An estimation of the "simulated" tilt angle of the fish during the change of observation angle is the sum of the observation angle, the swimming angle and the alongship angle from the split-beam echo sounder (Figure 3). The sign convention for the tilt angle is that a positive tilt angle denotes the head-towards-transducer or head-up attitude (Foote, 1980a). In order to correct the measured fish tilt angles, the estimated angles of the fish from the camera viewplane were used (for details, see Appendix B). Tilt angles for a fish at a specific depth

usually extended from about 10° to about -30°, but sometimes covered a greater tilt angle interval in the positive or negative direction (see Appendix C).

Measurements of TS at different tilt angles were performed at 5 and 20 m depths (n=10). Due to poor light conditions, only two capelin were measured at 5, 20 and 40 m depths.

When TS as a function of tilt angle for an individual fish is known, the mean backscattering cross section of a fish at a certain depth ($\sigma_{bs\ i}$) can be estimated at different tilt angle distributions of the fish (Foote, 1980a, 1980b). Thus $\sigma_{bs\ i}$ can be computed by using the probability density function (PDF) of fish tilt angle f(θ) as:

$$\sigma_{bs\ i} = \int_{\Delta\theta} \sigma(\theta')f(\theta')\partial\theta' \qquad (4)$$

where f(θ') is normalised over the range of tilt angle Δθ and σ(θ') is the angular function of the backscattering cross section of an individual fish.

According to Foote (1980b), the approximate normal tilt-angle distribution $N(\bar{\theta}, s\theta)$, where $\bar{\theta}$ is the mean tilt angle and sθ is the standard deviation, has the precise meaning given by the PDF:

$$f(\theta') = c^{-1} \exp[-(\theta' - \bar{\theta})^2/(2\, s\theta^2)] \quad \text{for } |\theta' - \bar{\theta}| \leq 3\, s\theta$$

$$= 0 \quad \text{for } |\theta' - \bar{\theta}| > 3\, s\theta \qquad (5)$$

where c^{-1} is a normalisation constant that equals 0.4 $s\theta^{-1}$.

$\sigma(\theta')$ values for tilt angles lying outside of the measuring range were occasionally needed in averaging computations. It has, however, been observed that $\sigma(\theta')$ values are often symmetric around a central angle (Foote, 1980c). This angle is usually negative (Blaxter and Batty, 1990), and is about –5° in capelin (Gauthier and Horne, 2002; Jørgensen, 2003). The angular range of $\sigma(\theta')$ was extended to the range needed in averaging computations by extrapolating $\sigma(\theta')$ values from the negative to the positive side (or vice versa) of a central angle of –5° (See Figure 4).

Maximum TS for each fish at a certain depth was defined as the mean backscattering cross section of the highest one percent of all ping values.

Estimating the contraction rate parameter (γ) and the constant b

In the method of fish abundance estimation by echo integration, the mean target strength (TS) is related to the average fish density (ρ_a) and the nautical area scattering coefficient (s_A) as:

$$s_A = \rho_a \times 4\pi \, 10^{0.1\,TS} \qquad \text{(MacLennan } \textit{et al.}\text{, 2002)} \qquad (6)$$

where a pressure independent mean TS for a fish with length L (cm) may be expressed as:

$$TS_0 = a \log_{10}(L) + b \qquad \text{(Nakken and Olsen, 1977)} \qquad (7)$$

If P = 1+z/10 is the pressure (atm) at depth z (m), a pressure dependent mean TS is expressed as:

$$TS = TS_0 + 10\gamma \log (P) \qquad \text{(Ona, 2003)} \qquad (8)$$

where TS and TS_0 are the mean target strengths at depth (z) and the surface, respectively.

Assuming the fish stay in an area during an echo survey, the logarithm of s_A at day compared to s_A at night gives an estimate of the change in mean TS (ΔTS).

$$10 \log(s_{Ad}/s_{An}) = \Delta TS \qquad (9)$$

By subtracting the TS values of day and night (equation 8), it follows that:

$$\gamma = \Delta TS /(10 \log_{10}(P_d/P_n)), \qquad (10)$$

where P_d is the pressure at the centre of the depth distribution at day and P_n is the pressure at the centre of the depth distribution at night. Combining equations 9 and 10 explains the relationship between γ, s_A and pressure during vertical migration:

$$\gamma = \log(s_{Ad}/s_{An})/\log(P_d/P_n) \qquad (11)$$

σ_{bs} at depth z can be expressed as:

$$\sigma_{bs\,z} = L^a\, 10^{0.1b}\, (P_z)^{\gamma} \qquad (12)$$

If (σ_{bs}) at depth z is approximately proportional with the square of the length where a = 2, then b is named b_{20} (Ona, 2003):

In order to normalise with fish length, the normalised backscattering cross section ($\sigma_{bs\ z}\ L^{-a}$, Haslett, 1965) can be estimated, usually with the parameter a equal to 2. When the parameters a, $\sigma_{bs\ z}$, L, P_z, and γ are known for a fish, the $10^{0.1b}$, and thus the corresponding b can be estimated.

Results

In 8 of the 10 capelin, lateral X-ray images showed that the swimbladder appeared to be intact with lengths ranging from 2.6 to 3.8 cm. Measurements of the swimbladders of the two other capelin were therefore rejected because gas was observed to have escaped into their oesophagus.

The acoustic backscattering cross section is shown to fluctuate with different tilt angles at all measuring depths. A plot of the observed backscattering directivity pattern of a 19.6-cm capelin is shown in Figure 4. Figure 5 shows a TS directivity pattern of the same capelin at 5, 20 and 40 m depths, respectively, where the TS values are based on σ_{bs} smoothed by using a probability density function (PDF) with a rather narrow tilt-angle distribution ($s\theta$ = 2.5°) around each tilt angle. The TS is observed to fluctuate with a distinct main lobe, but both the TS and its tilt-angle dependent fluctuations decrease at greater depths.

Figure 6 shows the estimated mean normalised backscattering cross section ($\sigma_{bs} L^{-2}$) of the capelin at 5, 20 and 40 m depths. The $\sigma_{bs} L^{-2}$ is shown to depend on the tilt-angle distribution. When the fish swim highly polarised (low $s\theta$), the $\sigma_{bs} L^{-2}$ vary more with respect to mean tilt angle than when the fish swim less polarised (higher $s\theta$). When the directivity diminishes at increasing depths, this effect also becomes reduced.

As shown in Figures 5 and 6, the estimated acoustic backscattering properties of capelin depend strongly on the ambient pressures. The change in mean TS and the corresponding contraction rate parameter (γ) during a descent from 5 to 20 m are given in Table 1. Also, the ranges of γ among different capelin individuals are given. As long as the swimming behaviour (tilt angle distribution) was identical at different depths, the mean TS always decreased with depth and the corresponding γ for individual capelin were negative. Changes in polarisation or mean tilt angle with depth caused variation in γ. Even positive γ is theoretically possible in extreme cases with strong vessel avoidance at night and lack of vessel avoidance during day.

The pressure dependence of σ_{bs} for different behavioural modes can be described by putting the parameters from Table 1 into equation 12. Thus, a σ_{bs} equation for capelin with behaviour as observed by Carscadden and Miller (1980) is given by:

$$\sigma_{bs\,z} = L^2\, 10^{-7.01} (P_z)^{-0.49}, (n=10) \qquad (13)$$

If we apply the length dependence proposed by O'Driscoll and Rose (2001) for capelin (5 to 14 cm), $\sigma_{bs\,z}$ can be normalised with $L^{-2.33}$. The contraction rate, γ, is virtually unchanged as compared to Table 1, while b is lower. With the behaviour observed by Carscadden and

Miller (1980), and the length dependence for capelin described by O'Driscoll and Rose (2001), the corresponding $\sigma_{bs\,z}$ and TS_z will be:

$$\sigma_{bs\,z} = L^{2.33}\ 10^{-7.43}\ (P_z)^{-0.49}, \qquad (14)$$

$$TS_z = 23.3\ \log_{10}(L) - 74.3 - 4.9\log_{10}(P_z) \qquad (15)$$

$23.3\ \log_{10}(L)$ length dependence and γ equal to –0.49 give a b-parameter of –74.3 dB with a 95% confidence interval from –73.7 to –75.0 dB.

Discussion

The experimental rig is used for estimating the effects of different tilt angles and ambient pressures on TS. One assumes that "simulating" a tilt angle of a fish by moving the transducer along the curved track is equivalent to a free-swimming fish changing the swimming direction vertically by a similar change of swimming tilt angle. A relevant question may be whether the shape of the swimbladder could be affected by the tilt angle. One can imagine that the swimbladder could become shorter and thicker when the fish was swimming upwards or downwards and get a more elongated shape when the fish was swimming horizontally. However, without changes in the gas volume, it seems unlikely that significant changes in the shape and length of the swimbladder can occur due to the more rigid structures of the body cavity surrounding the swimbladder, i. e. internal organs such as the liver, stomach, gonads and intestines.

Both theoretical and experimental evidence have been presented in support that the echo energy from schools or aggregations of fish is influenced by their behaviour. Such effects have also been quantitatively described as a result of different orientation distributions of the

fish (Foote, 1980b; Olsen, 1990; Gorska and Ona, 2003). As the results show, at 38 kHz the effect of tilt angle on mean TS is quite small for capelin (Jørgensen and Olsen, 2002; Jørgensen, 2003) in comparison to species such as herring or saithe (Foote, 1987b; Olsen and Ahlquist, 1996; Jørgensen, 1998). This is believed to be related to the difference between the swimbladder length and the wavelength of the transmitted sound at 38 kHz. This relation is usually smaller for capelin than for most other investigated species (Jørgensen, 2003; Gauthier and Horne, 2002).

The effect of mean tilt angle on mean TS, may, however, be strongly dependent on the degree of polarisation of the swimming behaviour, the size of the fish and the specimen's anatomy. Because the acoustic backscattering of capelin is shown less directive with respect to tilt angle, the dependence upon polarisation is also less pronounced in 18-cm capelin than in 23-cm saithe (see Figure 7). Further, an important effect of this fact is that a variation in tilt-angle distribution in capelin should be expected to have a less pronounced effect on the acoustic backscattering of capelin compared to fish with longer swimbladders. In Figure 7 (upper panels), this is demonstrated most clearly when comparing the normalised backscattering cross section of capelin with the one of saithe. However, when the acoustic backscattering cross section is normalised with the square of the swimbladder length, a more similar level among capelin and saithe is shown (Figure 7, lower panels).

Horne and Clay (1998) recommend frequencies to be chosen to restrict values of the ratio of total length of a target to the acoustic wavelength (L/λ) from 2 to 10. As L/λ increases, the influence of tilt angle on TS generally increases. The influence of tilt angle on TS is, however, indirectly related to the total length because only a limited part of the fish body, the swimbladder, is the major source of the backscattered sound (Foote, 1980d). The L/λ of the

saithe in Figure 7 ranges from 5.8 to 6.0, only about 30 % higher than in the capelin, which have L/λ from 4.5 to 5.0. However, the ratio between swimbladder length and the acoustic wavelength at 38 kHz (SBL/λ) of the saithe is from 2.1 to 2.2, more than twice as high as in the capelin (SBL/λ from 0.7 to 1.0).

In a similar manner, the lesser maximum TS of capelin, as compared to saithe of similar size, is explained by differences in the ratio between the swimbladder length and the total length of the capelin (0.15 to 0.19) and the saithe (0.34 to 0.37). This is visualised in Figure 8 where data on maximum TS of 8 capelin and 5 saithe are merged. Only 22% of the variation in maximum TS is explained by linear regression with the logarithm of length as independent variable, whereas 98% of the variation is explained by linear regression with the logarithm of swimbladder length as independent variable.

For some fish species with physostomous swimbladders, it has been shown that TS does not recover even if the fish remain at the same depth for some time (Mukai and Iida 1996; Ona, 2003). On the basis of morphological investigations, Fáhlen (1968) proposed that no gas secretion occurs in the swimbladder of capelin. The results presented in this paper suggest that capelin TS is strongly negatively related to pressure. The estimate of the contraction rate parameter was about –0.5 to –0.6 for capelin in this experiment, which is close to the –0.67 expected from Boyle's Law. It should, however, be emphasised that no studies were undertaken to investigate whether a prolonged time during the depth excursions can influence the swimbladder compression, as was indicated in an experiment with a related physostomous species, Arctic charr, *Salvelinus alpinus* (Sundnes and Bratland, 1972).

Table 2 shows changes in maximum TS with depth (ΔTS_{max}) and the corresponding contraction rate (γ_{max}) for three different species measured in the submersible rig. γ_{max} from 5 to 20 m depths for the three species was not equal (Kruskal-Wallis test, p=0.002). The Kruskal-Wallis test with multiple comparisons with unequal sample sizes (Zar, 1998) show that the γ_{max} of capelin was significantly different from saithe ($Q = 3.5$, $p<0.002$). The γ_{max} of capelin tended to be lower than the one for herring, but the difference was not significant at the 0.05 level (Kruskal-Wallis test, $Q = 2.2$, $0.05<p<0.1$). The γ_{max} of saithe was not significantly different from that of herring (Kruskal-Wallis test, $Q = 0.79$, $p>0.5$).

The depth dependence of maximum TS of capelin is negative and tend to be stronger than observed in herring and in under-buoyant saithe. Mathematical models of the acoustic backscattering from gas bladders (Clay, 1992) demonstrate that if the swimbladder is shortened by a decrease in gas volume, this leads to a much more dramatic decrease in maximum TS than if the width is decreased due to the loss of a similar gas volume (Jørgensen, 1998). Thus, the differences in depth dependence of maximum TS might arise from differences in swimbladder physiology among capelin, herring and saithe. The relatively long and slender gas bladder of the physoclistous saithe is attached to the vertebra column and the long and slender gas bladder of the physostomous herring is stretched out between the anterior bullas and the posterior anal duct (Blaxter and Tytler, 1978). When an increased pressure decreases the volume of these gas bladders, the two designs might lead to compression in width rather than in length (Ona, 1990; Gorska and Ona, 2003). The shorter gas bladder of the physostomous capelin does not possess an anal duct and is loosely attached to the surrounding organs. It is, however, firmly attached anteriorly to the oesophagus (Fahlén, 1968). It might therefore be more easily compressed in length than the gas bladder of herring and saithe, leading to a stronger depth dependence of maximum TS of capelin.

The contraction rate (γ) is based on changes in mean TS and is thus affected by the gas producing capabilities of the fishes plus changes in pressure and tilt-angle distribution. In contrast, the contraction rate based on maximum TS, (γ_{max}), is independent of the tilt-angle distribution. γ as defined by Ona (2003) may be viewed as a pressure-dependent correction rate for the mean backscattering cross section that is usually negative. However, the hypothetical simulations with capelin show that γ in theory can also attain positive values in some situations if vessel avoidance leads to strong diving behaviour at shallow depth at night, but little or no avoidance behaviour takes place at greater depths during the day. This rather extreme situation would lead to an increase in the mean TS at greater depths even though the maximum TS decreased with depth. For fish where the influence of tilt angle on TS is stronger than in capelin, e.g. mature herring and gadoids (Nakken and Olsen, 1977), a positive γ may also possibly appear at less extreme diving behaviour than that required to demonstrate this effect in capelin.

The negative depth dependence of capelin TS observed in this study is supported by the findings of Shackell *et al.* (1994). Acoustic estimates of capelin density in Canadian waters were observed to be greater at night at rather shallow depth (20-100 m) than at deeper depths (101-192 m) during day, and the average ratio of deep to shallow densities was 1:3.5 (Shackell *et al*., 1994). Gjøsæter and Jørgensen (unpublished data) observed a twofold day-night increase in s_A of capelin in a small area in the Barents Sea following a diurnal cycle. The capelin performed vertical migration with a centre of the depth distribution of 138 m at daytime and 34 m at nighttime. Aglen (1989), however, observed no significant difference between total average integrator values for capelin in the Barents Sea (corresponds to s_A) obtained during day and night.

Shackell *et al.* (1994) stated that TS might be modified by changes in swimbladder volume, but favoured the hypothesis that depth-related densities were caused by different orientations during the day and at night. At 38 kHz, however, the drop in TS attributable to changes in tilt angle is expected to be rather small for a relatively omnidirectional backscattering target such as a capelin (Olsen and Angell, 1983; Olsen and Ahlquist, 1989; Jørgensen and Olsen, 2002; Jørgensen, 2003), especially at greater depths as has previously been shown in Figure 6.

The TS equation used in the Barents Sea capelin surveys today (equation 2) would be expected to give lower values than the depth-dependent TS from equation 15 at rather shallow depth, but higher values at greater depths. Thus, as a consequence of differences in depth distributions and fish sizes, fish density estimated by using commonly used TS equations for capelin (Toresen *et al*., 1998; O'Driscoll and Rose, 2001) may be expected to be overestimated at rather shallow depths and underestimated at greater depths.

The equations for capelin presented in this paper need to be verified or corrected by *in situ* and *ex situ* TS measurements that cover a range in depths and fish lengths representative of the vertical distribution and length distributions of the acoustic survey of the Barents Sea capelin. However, it is strongly recommended to include the effects of ambient pressure into the TS equation used for survey purposes because the acoustic stock size estimate of capelin in the Barents Sea is regarded as an absolute estimate of stock abundance.

Acknowledgements

Special thanks are due to Captain Arnfinn Utheim and his crew on board the research vessel "Johan Ruud" that took part in the surveys and made these experiments possible. We are

grateful to them for their invaluable help and great patience during the experiments with the submersible rig. We are also grateful to Otto Ottesen and Hermod Ditlefsen for catching the saithe used in the testing of the rig. Our thanks to Gunvald Wagelid, Eilert Halsnes and Asle Balsvik for helping with preparing and fixing the experimental rig prior to and after the experiments. And our gratitude to Jørgen S. Christiansen, Kim Præbel and Bjørn S. Sæther (NCFS) for keeping the capelin in tanks and providing live material and X-ray pictures.

References

Aglen, A. 1989. Echo integrator threshold and fish density distribution. In Reliability of acoustic fish abundance. *In* Reliability of acoustic fish abundance estimates. Dr. scient. thesis. University of Bergen, Norway. pp 59-77.

Blaxter, J.H.S., and Batty, R.S., 1990. Swimbladder "behaviour" and target strength. Rapports et Procès-Verbaux des Rèunions du Conseil International pour l`Exploration de la Mer, 189: 233-244.

Blaxter J.H.S., and Tytler, P. 1978. Physiology and function of the swimbladder. Advances in Comparative Physiology and Biochemistry, 7: 311-367.

Carscadden, J.E., and Miller, D.S. 1980. Estimates of tilt angle of capelin using underwater photographs. ICES C.M. 1980/H:50. 7 pp.

Carscadden, J.E., and Vilhjálmsson, H. 2002. Capelin – What Are They Good For? Introduction. ICES Journal of Marine Science, 59: 863-869.

Clay, C.S. 1992. Composite ray-mode approximations for backscattered sound from gas-filled cylinders and swimbladders. The Journal of the Acoustical Society of America, 92: 2173-2180.

Dalen, J., Raknes, A., and Røttingen, I. 1976. Target strength measurements and acoustic biomass estimation of capelin and 0-group fish. ICES C.M. 1976/B:37. 18 pp.

Dommasnes, A., and Røttingen, I. 1984. Acoustic stock measurements of the Barents Sea capelin 1972-1984, a review. Pp 45-63 *in:* H. Gjøsæter (ed.) The Proceedings of the Soviet-Norwegian Symposium on the Barents Sea Capelin, Bergen, Norway, 14-17 August 1984. Institute of Marine Research, Norway, 236 pp.

Fahlén, G. 1968. The gas bladder as a hydrostatic organ in *Thymallus thymallus* L., *Osmerus eperlanus* L. and *Mallotus villosus* Müll. Fiskeridirektoratets Skrifter Serie Havundersøkelser, 14: 199-228.

Foote, K.G. 1980a. Averaging of fish target strength functions. The Journal of the Acoustical Society of America, 67: 504-515.

Foote, K.G. 1980b. Effect of fish behaviour on echo energy: the need for measurements of orientation distributions. Journal du Conseil International pour l'Exploration de la Mer, 39: 193-201.

Foote, K.G. 1980c. Angular measures of dorsal aspect target strength functions of fish. Fiskeridirektoratets Skrifter Serie Havundersøkelser, 17: 49-70.

Foote, K.G. 1980d. Importance of the swimbladder in acoustic scattering by fish: a comparison of gadoid and mackerel target strength. The Journal of the Acoustical Society of America, 67: 2084-2089.

Foote, K.G. 1987a. Fish target strengths for use in echo integrator surveys. The Journal of the Acoustical Society of America, 82: 981-987.

Foote, K.G. 1987b. Target strength of polarized fish. ICES CM 1987/B:4, 10 pp.

Gauthier, S., and Horne, J.K. 2002. Species-specific differences in acoustic properties of Bering Sea and Gulf of Alaska forage fish. Manuscript. ICES Symposium Acoustics in Fisheries and Aquatic Ecology, Montpellier, France, 10-14 June 2002. 12 pp.

Gjøsæter, H. 1998. The population biology and exploitation of capelin (*Mallotus villosus*) in the Barents Sea. Sarsia, 83: 453-496.

Gjøsæter, H, Bogstad, B., and Tjelmeland, S. 2002. Assessment methodology for Barents Sea capelin (*Mallotus villosus* Müller). ICES Journal of Marine Science, 59:1086-1095.

Gorska, N., and Ona, E. 2003. Modelling the effect of swimbladder compression on the acoustic backscattering from herring at normal or near-normal dorsal incidences. ICES Journal of Marine Science, 60:1381-1391.

Haslett, R.W.G. 1965. Acoustic backscattering cross sections of fish at three frequencies and their representation on a universal graph. British Journal of Applied Physics, 16: 1143-1150.

Horne, J.K., and Clay, C.S. 1998. Sonar systems and aquatic organisms: matching equipment and model parameters. Canadian Journal of Fisheries and Aquatic Sciences, 55: 1296-1306.

Jørgensen, R. 1998. Eksperimentell måling av akustisk tilbakespredning fra sei (*Pollachius virens* L.): Et studie av metodiske spørsmål i tilknytning til akustisk fiskemengdemåling. Master thesis. The Norwegian College of Fishery Science, University of Tromsø, Norway. 124 pp.

Jørgensen, R. 2003. The effects of swimbladder size, condition and gonads on the acoustic target strength of mature capelin. ICES Journal of Marine Science, 60: 1056-1062.

Jørgensen, R., and Olsen, K. 2002. Acoustic target strength of capelin measured by single target tracking in a controlled cage experiment. ICES Journal of Marine Science, 59: 1081-1085.

MacLennan, D.N., Fernandes, P.G., and Dalen, J. 2002. A consistent approach to definitions and symbols in fisheries acoustics. ICES Journal of Marine Science, 59: 365-369.

Midttun, L., and Nakken, O. 1971. On acoustic identification, sizing and abundance estimation of fish. Fiskeridirektoratets Skrifter Serie Havundersøkelser, 16: 36-48.

Midttun, L., and Nakken, O. 1977. Some results of abundance estimation studies with echo integrators. Rapports et Proce`s-Verbaux des Re´unions du Conseil International pour l'Exploration de la Mer, 170: 253-258.

Mukai, T., and Iida, K. 1996. Depth dependence of target strength of live kokanee salmon in accordance with Boyle's Law. ICES Journal of Marine Science, 53: 245-248.

Nakken, O., and Olsen, K. 1977. Target strength measurements of fish. Rapports et Procès-Verbaux des Rèunions du Conseil International pour l`Exploration de la Mer, 170: 52-69.

O'Driscoll, R.L., and Rose, G.A. 2001. *In situ* target strength of juvenile capelin. ICES Journal of Marine Science, 58: 342-345.

Olsen, K. 1990. Fish behaviour and acoustic sampling. Rapports et Procès-Verbaux des Réunions du Conseil International pour l`Exploration de la Mer, 189: 147-158.

Olsen, K., and Ahlquist, I. 1989. Target strength of fish at various depths, observed experimentally. ICES C.M. 1989/B:53. 8 pp.

Olsen, K., and Ahlquist, I. 1996. Target strength of herring at depth. ICES C.M. 1996/B:27. 12 pp.

Olsen, K., and Angell, J. 1983. A comparison of different echo abundance conversion methods. ICES CM 1983/B:17. 12 pp.

Ona, E. 1990. Physiological factors causing natural variations in acoustic target strength of fish. Journal of the Marine Biological Association of the United Kingdom, 70: 107-127.

Ona, E. 2003. An expanded target-strength relationship for herring. ICES Journal of Marine Science, 60: 493-499.

Shackell, N.L., Carscadden, J.E., and Miller, D.S. 1994. Diel vertical migration of capelin (*Mallotus villosus*) and its effect on acoustic estimates of density. ICES C.M. 1994/Mini: 5. 18 pp.

SIMRAD. 1999. SIMRAD EY500 Portable Scientific Echo Sounder (Version 5.33). Instruction manual. SIMRAD AS, Horten, Norway (1999). 243 pp.

Sundnes, G., and Bratland, P. 1972. Notes on the gas content and neutral buoyancy in physostome fish. Fiskeridirektoratets Skrifter Serie Havundersøkelser, 16: 89-97.

Toresen, R., Gjøsæter, H., and de Barros, P. 1998. The acoustic method as used in the acoustic abundance estimation of capelin (*Mallotus villosus* Müller) and herring (*Clupea harengus* Linné) in the Barents Sea. Fisheries Research, 34: 27-37.

Zar, J. H. 1998. Biostatistical Analysis, 4th Edition. Prentice-Hall, New Jersey. 663 pp.

Table 1: Estimated mean contraction rate parameter (γ) for capelin (n=10) when descended from 5 to 20 m depth computed from the change in target strength and from different hypothetical tilt-angle distributions. Tilt-angle distributions are the observations of Olsen and Angel $(1983)_1$, Jørgensen $(2003)_2$, and Carscadden and Miller $(1980)_3$. In addition, the results of a change in schooling behaviour during vertical migration are estimated, simulated with different tilt-angle distributions at 5 m (N(0, 20)) and 20 m (N(5, 10)). Further given are the hypothetical results of moderate avoidance behaviour at 5 m at nighttime and undisturbed at 20 m in daytime ($N(-16.5, 8.6)_{5m}$ and $N(3.3, 18.4)_{20m}$), or strong avoidance at nighttime but horizontal swimming with the same polarisation at 20 m in daytime ($N(-25, 10)_{5m}$, $N(0, 10)_{20m}$). ΔTS is computed from the mean change in $\sigma_{bs}\, L^{-2}$. Estimated b_{20} is also given.

Tilt-angle distribution (°)	γ		ΔTS	b_{20}
	Mean	Total range	(dB)	(dB)
$N(-16.5, 8.6)_1$	-0.63	-0.34 to –0.81	-1.89	-69.3
$N(3.2, 4.8)_1$	-0.52	-0.24 to –0.83	-1.57	-68.7
$N(-3, 13)_2$	-0.56	-0.39 to –0.77	-1.69	-69.1
$N(3.3, 18.4)_3$	-0.49	-0.26 to –0.73	-1.47	-70.1
Change in schooling behaviour	-0.25	-0.06 to –0.48	-0.74	-70.6
Moderate avoidance	-0.67	-0.43 to –0.88	-2.02	-69.2
Strong avoidance	0.17	0.65 to –0.22	0.52	-72.3
Maximum TS	-0.57	-0.29 to –1.0	-1.72	-66.1

Table 2: Changes in maximum TS (ΔTS_{max}) with depth and the corresponding contraction rate (γ_{max}) for three different species measured in a submersible rig.

	Depth (m)		ΔTS_{max}	γ_{max}		n	Reference
	Min.	Max.	(dB)	Mean	Total range		
Capelin	5	20	-1.8	-0.57	-0.29 to –1.0	10	Present study
	5	40	–3.3 and -4.1		-0.63 and –0.79	2	Present study
Saithe	5	20	-0.59	-0.20	-0.03 to –0.41	5	Present study
	5	20	-0.91	-0.30	-0.24 to –0.34	6	Jørgensen (1998)
	5	50	-1.24	-0.21		1	
Herring	5	20	-1.0	-0.35	-0.10 to –0.56	6	Olsen and
	5	50	-1.9	-0.34	-0.15 to –0.58	5	Ahlquist (1996)

Figure legends

Figure 1: Side view of the measuring rig (A) and a more detailed view of the cage arrangement in front aspect (B). The fish cage (1) is positioned in the centre of the acoustic beam from the SIMRAD ES 38-12 transducer (2). Underwater television (3) enables the fish behaviour (aspect angle) with reference to a vertical steel tube (4) to be monitored. The cage is held in position by a system of nylon gut suspension (5) attached to the rig, the steel tubes and a steel ring (6). Different observation angles are obtained when the transducerwagon is moved along the curved track (7) by a winch (8) combined with a weight (9). The current due to the towing speed (10) is monitored by a current meter (11). The measuring rig is stabilised by a rudder (12) and can be suspended by a wire (13) from the vessel derrick.

Figure 2: The target strength of the copper sphere compared to the target strength of the cage.

Figure 3. Relationship between time, simulated tilt angle, observation angle, swimming angle and alongship off axis angle during a measuring sequence for a fish with rather positive (head up) swimming angle.

Figure 4. Extrapolation of $\sigma(\theta)$ values from the negative to the positive side of the $\sigma(\theta)$ function assuming a central angle of –5° and an approximately symmetric $\sigma(\theta)$ function. The measured $\sigma(\theta)$ values (n = 2737) are in black and the extrapolated parts of the $\sigma(\theta)$ function are in red. The vertical dashed lines show the central angle (middle) and the lower and higher limits of the "symmetric" $\sigma(\theta)$.

Figure 5: TS plotted against tilt angle for a 19.6-cm capelin at 5-m depth (solid line), 20-m depth (dashed line) and 40-m depth (dotted line).

Figure 6: Mean normalised backscattering cross section (σ_{bs} L^{-2}) normalised to the square of the length plotted against mean tilt angle with high degree of polarisation ($s\theta$=2.5° and 5°), and medium ($s\theta$=10°) and low ($s\theta$=20°) degree of polarisation in swimming behaviour. The curved solid line shows mean $\sigma_{bs}L^{-2}$ values for capelin at 5 m depth and the dashed line shows the corresponding mean $\sigma_{bs}L^{-2}$ at 20-m depth (n=10). The dotted line shows mean $\sigma_{bs}L^{-2}$ values for two capelin at 40-m depth.

Figure 7: Mean backscattering cross section (σ_{bs}) at 5-m depth normalised to the square of the length (L^2) plotted against mean tilt angle with higher ($s\theta$=2.5°) and lower ($s\theta$=10°) degree of polarisation in swimming behaviour. The solid line shows the corresponding mean $\sigma_{bs}L^{-2}$ for 10 capelin (17.5 to 19.6 cm), and the dashed line shows mean $\sigma_{bs}L^{-2}$ values for three saithe (22.4 to 23.4 cm).

Figure 8: Maximum TS of capelin (cross) and saithe (circle) plotted against the logarithm of total length (left panel) and swimbladder length (right panel).

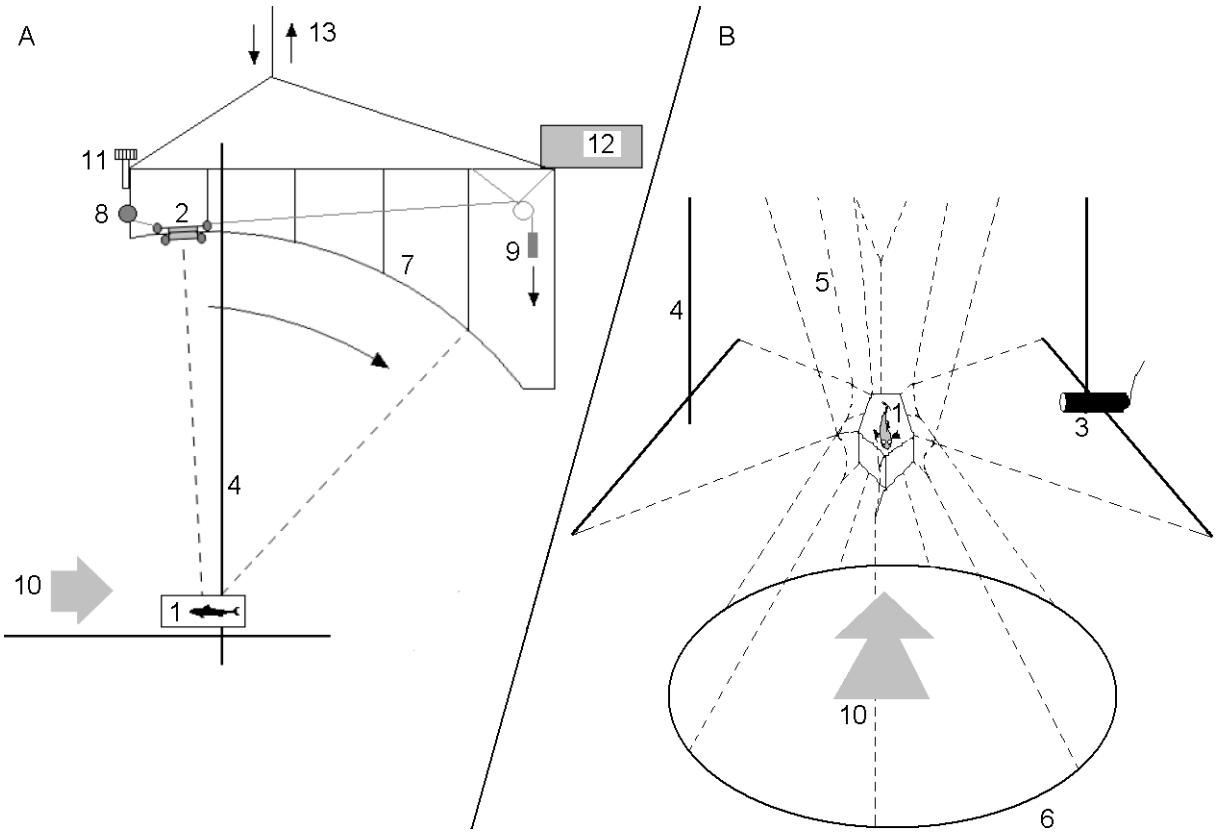

Figure 1

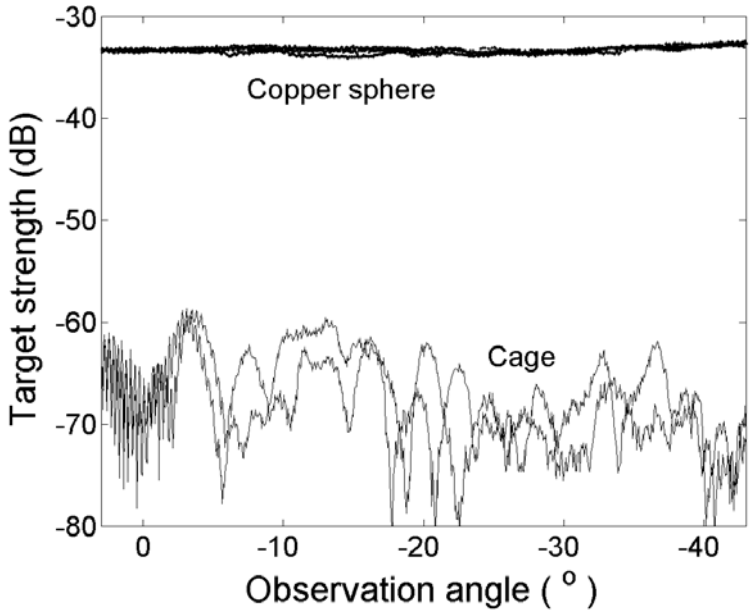
-30
-40
-50
-60
-70
-80
Target strength (dB)
Copper sphere
Cage
0
-10
-20
-30
-40
Observation angle (o)

Figure 2

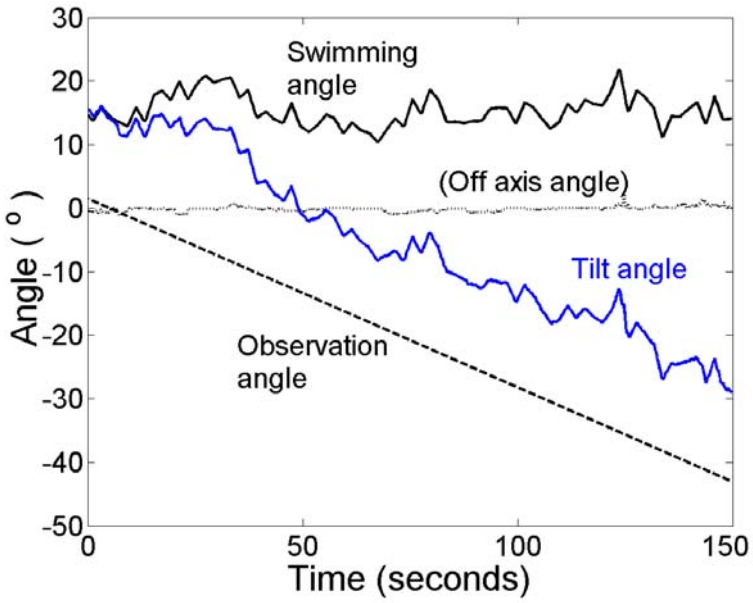
Swimming
angle
(Off axis angle)
Tilt angle
Observation
angle
Angle (°)
Time (seconds)
30
20
10
0
-10
-20
-30
-40
-50
0
50
100
150

Figure 3

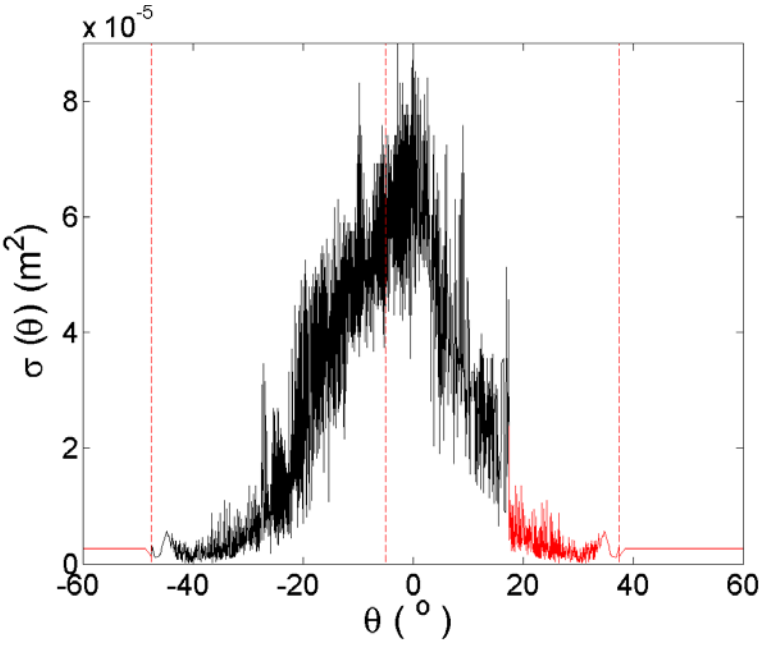

Figure 4

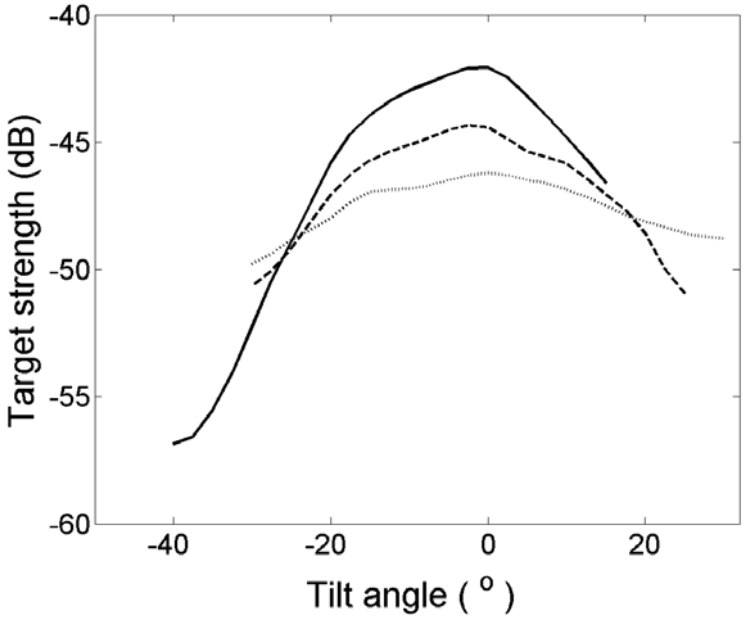

Figure 5

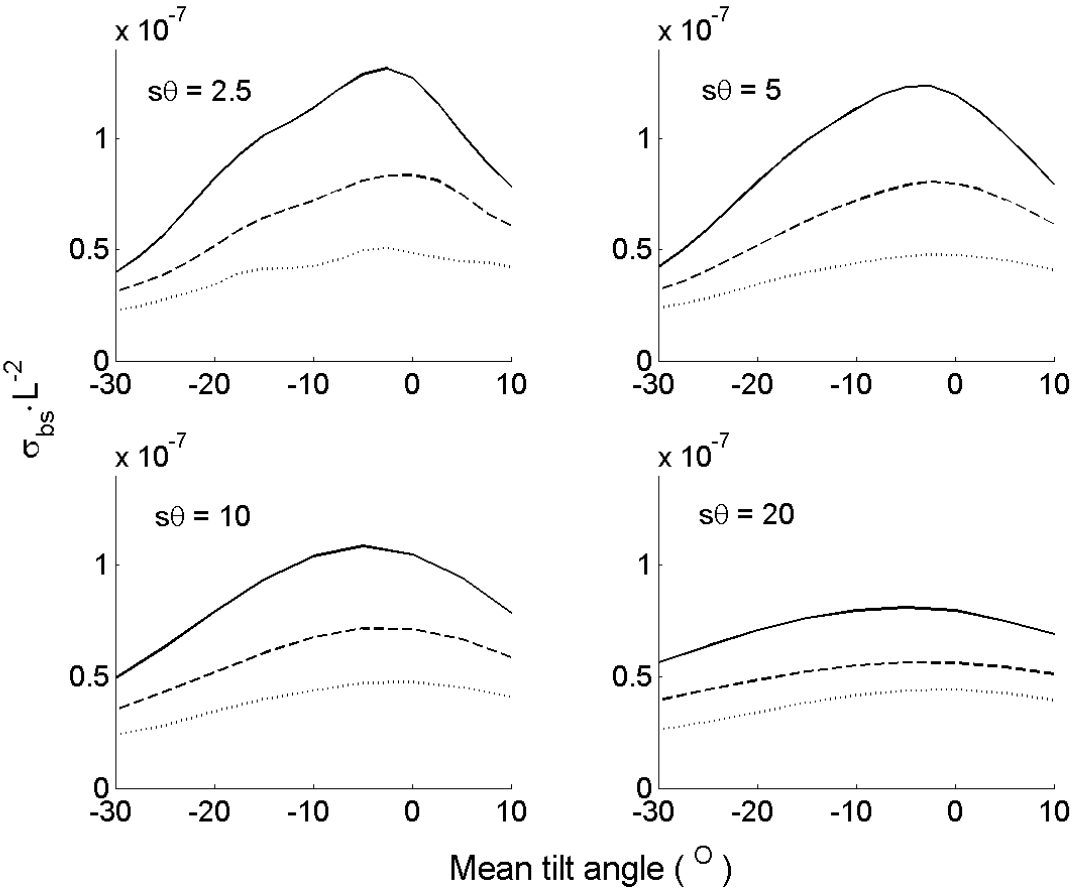

Figure 6

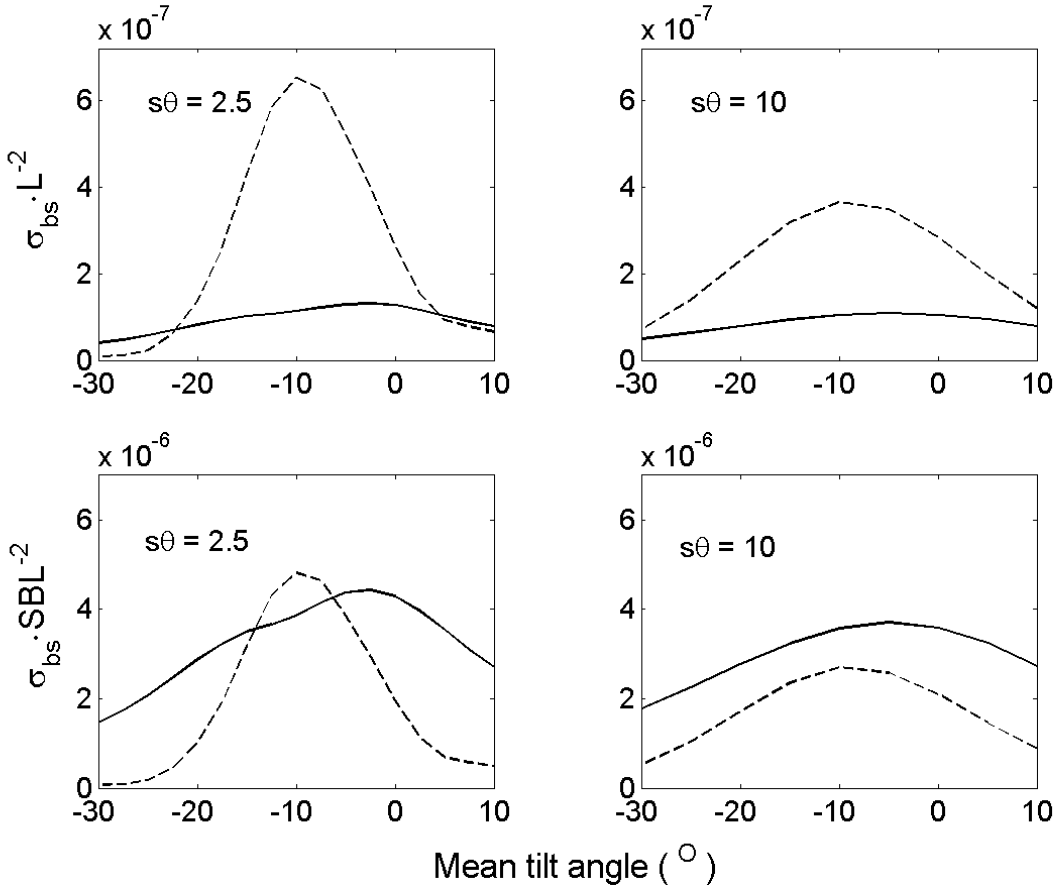
x 10^-7
sθ = 2.5
σbs·L^-2
x 10^-7
sθ = 10
x 10^-6
sθ = 2.5
σbs·SBL^-2
x 10^-6
sθ = 10
Mean tilt angle (O)

Figure 7

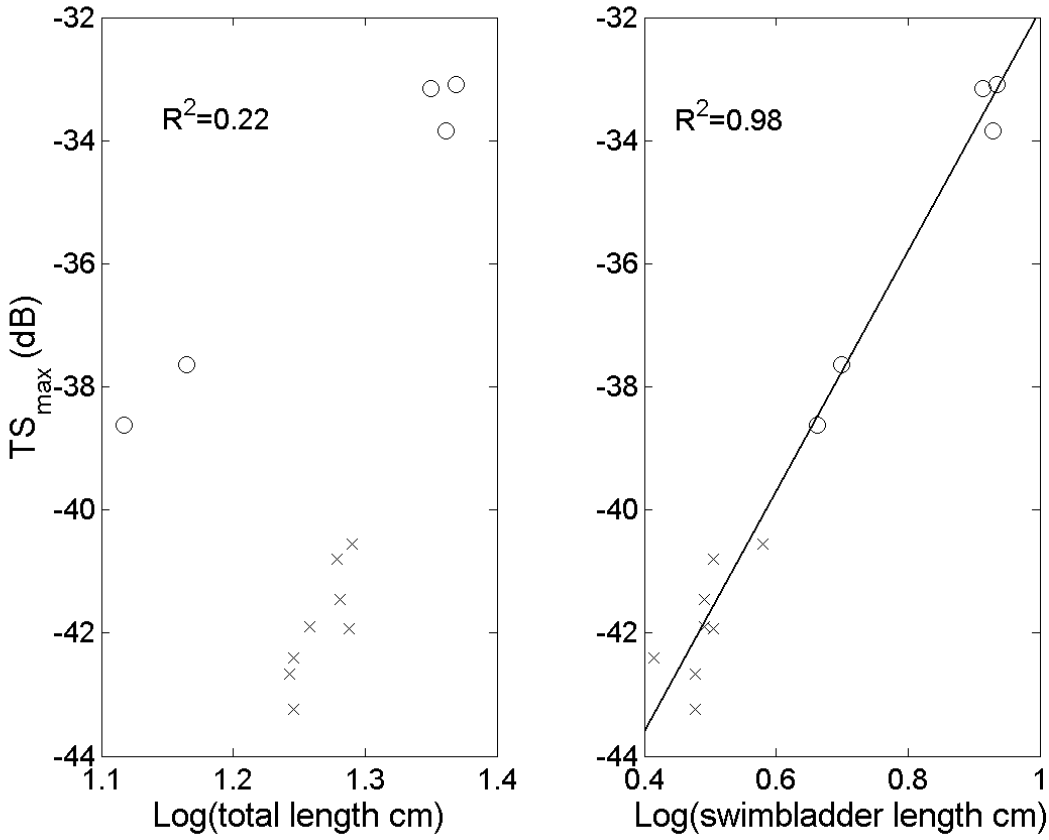
-32
-34
-36
-38
-40
-42
-44
TS max (dB)
R2=0.22
1.1
1.2
1.3
1.4
Log(total length cm)
R2=0.98
0.4
0.6
0.8
1
Log(swimbladder length cm)

Figure 8

Appendix A

Table A: Performance tests in the actual measuring situation in the rig performed at 5, 20 and 40 m depths for the copper sphere, the empty cage or with no cage. The deviation between the theoretical TS value of the copper sphere (-33.6 dB) and the TS measured by the calibrated split beam echo sounder is given. TS values of the cage are estimated from the volume backscattering coefficient of the cage and the copper sphere.

Date	Target	Depth (m)	$\sigma_{bs} \pm$ sd σ_{bs} (10^{-5} m^2)	TS (dB)	Deviation (dB)	n
22.10. 01	No cage	5	0.005±0.006	-73.0		1510
	Cage	5	0.075±0.09	-61.2		1541
	Copper sphere	5	44.7±2.4	-33.5	-0.1	3761
14.05.02	Cage	5	0.075±0.08	-61.2		1555
	Cage	20	0.033±0.04	-64.8		3024
	Cage	5	0.029±0.03	-65.4		1532
	Copper sphere	20	41.9±2.8	-33.8	0.2	2565
	Copper sphere	40	38.5±2.3	-34.1	0.5	2568
	Copper sphere	5	47.0±3.1	-33.3	-0.3	2584

Appendix B

Estimating the swimming angle

In order to estimate changes in the swimming angle of the fish, the coordinates of the tip of the upper jaw (x_1, y_1), the root of the tail (x_2, y_2) and the higher (x_3, y_3) and lower (x_4, y_4) part of the steel tube were measured from videotape images. During these operations, video processing software (Pinnacle Systems Inc.) and MATLAB image processing software (Math Works Inc.) were used. Coordinates from images were measured with two-second intervals, which corresponds to 1.2 images per degree change in observation angle. In order to filtrate out measurement sequences where the fish did not perform a sufficiently regular swimming behaviour, no values ("NaN" in MATLAB language) were assigned to coordinates from sequences where the fish turned around or were resting on the net cage "floor".

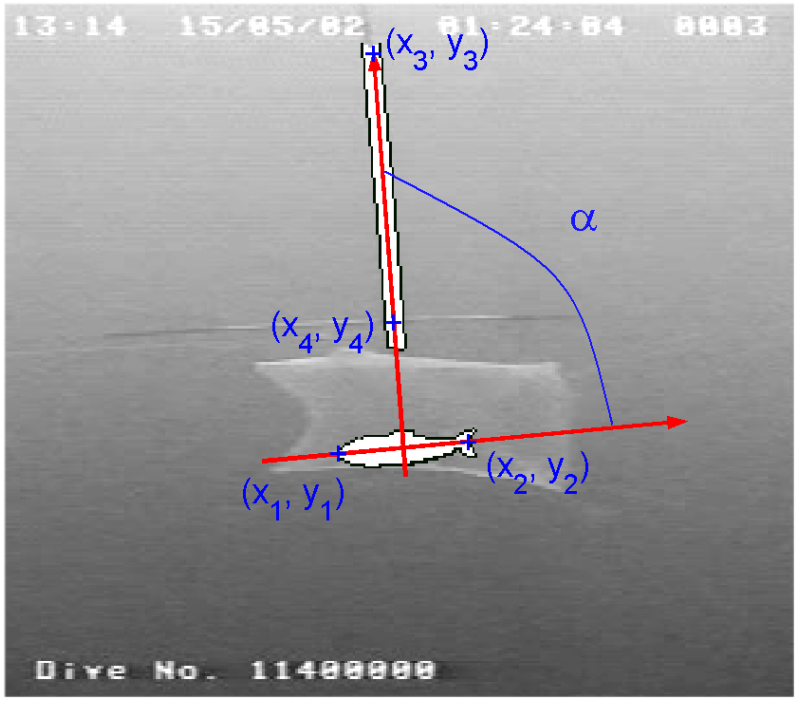

Figure B1: Coordinates and the angle (α) between the fish and the vertical steel tube. A video image of the cage is used as background.

Subtracting 90° from the angle (α) between the fish and a vertical steel tube calculates the observed swimming angle of the projection of the fish in the camera viewplane. The observed swimming angles (v_{obs}) were computed from the coordinates in Figure B1 using the dot product between the vector going through the fish (l) and the vector going through the vertical steel rod (t):

$$v_{obs} = \alpha - 90^{\circ} = \arccos\left(\frac{l \cdot t}{|l| \cdot |t|}\right) - 90^{\circ} \qquad \text{(B1)}$$

If the fish is swimming at an angle to the camera viewplane, observed swimming angles other than 0° will be underestimated for negative and overestimated for positive swimming angles.

v_{obs} is the projection of the real swimming angle (v) in the camera viewplane. v was computed using the formula:

$$v = v_{obs} - \arcsin\left(\frac{y_1 - y_2}{|l_{obs}|}\right) + \arcsin\left(\frac{y_1 - y_2}{|l_{\max}|}\right) \qquad \text{(B2)}$$

where $|l_{obs}|$ is the measured length of the fish in the camera viewplane and $|l_{max}|$ is the maximal observed length of the fish.

Nakken and Olsen (1977) showed that changes in roll angle of ± 40° apparently did not affect TS of herring or saithe. In the rig experiment, the video images and the corresponding TS

measurements were rejected if the lateral surface of a fish was not within 37° of the camera viewplane. When the lateral surface of a fish is outside 37° of the camera viewplane, the cosine of the ratio of the observed fish length projection to the real (maximum) fish length (the ratio of $|l_{obs}|$ to $|l_{max}|$) is less than 0.8. A scrutinising program written in MATLAB used the ratio of $|l_{obs}|$ to $|l_{max}|$ equal to 0.8 as the limit value under which the coordinates from the images and the corresponding TS measurements were not assigned a value ("NaN").

References

Nakken, O., and Olsen, K. 1977. Target strength measurements of fish. Rapports et Procès-Verbaux des Rèunions du Conseil International pour l`Exploration de la Mer, 170: 52-69.

Appendix C

Table C: Overview of some measured values for the fish used in the rig experiment. The total lengths and swimbladder lengths (SBL) are given. Capelin where a significant amount of gas had escaped from the swimbladder into the oesophagus is given no swimbladder length and marked OE. Also given is time from the fish was submerged to the first measuring depth until the TS measurements started or stopped. The maximum range in tilt angles is given for each depth for all the capelin measurements and for some saithe measurements. The maximum target strength (TS) in decibel is given.

	Length (cm)	SBL (cm)	Depth (m)	Time (min)		Tilt angle (°)			TS (dB)	
				Start	Stop	Max	Min	n	Max	n
Capelin										
C01	19.4	3.2	20	10	27	6.7	-53.3	127	-42.8	1271
			5	32	44	18.0	-55.7	246	-41.9	2456
C02	19.5	3.8	20	10	28	33.3	-25.9	291	-42.3	2912
			5	70	73	24.7	-30.4	72	-40.5	716
C03	19.0	3.2	20	10	20	20.8	-42.3	173	-42.1	1730
			5	38	47	20.5	-35.8	157	-40.8	1566
C04	18.1	OE	20	10	21	13.0	-51.3	217	-44.3	2170
			5	26	37	15.4	-36.2	102	-42.3	1018
C05	19.1	3.1	20	10	16	12.3	-54.7	140	-43.1	1403
			5	69	73	-0.8	-53.3	46	-41.5	458
C06	17.5	3.0	20	10	19	19.2	-25.8	134	-43.7	1337
			5	36	57	29.0	-30.6	174	-42.7	1736
C07	18.1	3.1	20	10	19	18.4	-47.0	139	-43.5	1389
			5	26	49	24.3	-59.8	79	-41.9	789
C08	19.6	OE	20	10	18	25.8	-30.5	222	-43.1	2217
			40	26	35	30.7	-31.8	226	-45.0	2257
			5	42	60	17.5	-47.5	302	-40.9	3018
C09	17.6	3.0	5	10	16	29.1	-28.3	104	-43.2	1038
			20	25	30	48.9	-24.9	116	-46.3	1160
C10	17.6	2.6	5	10	23	16.8	-44.9	274	-42.4	2737
			20	30	42	18.3	-41.0	277	-44.7	2774
			40	47	59	12.4	-42.7	196	-45.7	1959
Saithe										
S01	23.4	8.6	5	10	13	9.1	-46.1	76	-33.1	760
			20	30	33				-33.8	730
S02	23.0	8.5	5	10	16	8.2	-52.4	147	-33.8	1466
			20	35	41				-33.9	1436
S03	22.4	8.2	5	10	16	15.6	-42.5	140	-33.2	1402
			20	59	62				-34.4	768
S04	13.1	4.6	5	10	16				-38.6	1511
			20	31	38				-38.9	1507
S05	14.6	5.0	5	10	17				-37.6	1502
			20	33	39				-38.2	1490

Twisting and turning

The old pine tree
by the grandmother house
watches the fjord
- twists against the sun

But the grandfather clock
turns in the opposite
direction

Some fishermen and hunters
seldom turned their boat
against the sun
even if they had to travel
almost the full circle

Vri og dreie

Dein gamle forra
atme bæstemorhuse
speide over fjord'n
- vrir seg mot sola

Men bæstefarklokka
går i motsatt retning

Nån feskera og fangstfolk
dreide sjelden båtn mot sola
sjøl om dem måtte fullføre
nesten heile sirkelen